

Snakes and isolas in non-reversible conservative systems

Björn Sandstede

Division of Applied Mathematics
Brown University
Providence, RI 02912, USA

Yancong Xu

Department of Mathematics
Hangzhou Normal University
Zhejiang 310036, People's Republic of China

April 29, 2012

Abstract

Reversible variational partial differential equations such as the Swift–Hohenberg equation can admit localized stationary roll structures whose solution branches are bounded in parameter space but unbounded in function space, with the width of the roll plateaus increasing without bound along the branch: this scenario is commonly referred to as snaking. In this work, the structure of the bifurcation diagrams of localized rolls is investigated for variational but non-reversible systems, and conditions are derived that guarantee snaking or result in diagrams that either consist entirely of isolas.

1 Introduction

Localized roll structures such as the ones shown in Figure 1 arise in many physical processes: examples are buckling patterns in struts, localized convection rolls in fluids, and optical light patterns in lasers and gas-discharge systems, and we refer to [1, 6, 9] for references and additional applications. In many cases, the solution branches of localized roll patterns are unbounded in function space but bounded in parameter space, and a typical bifurcation diagram and sample solution profiles are shown in Figure 1: note that the width of the roll plateau increases along the solution branch, leading to an unbounded L^2 -norm, and this scenario is often referred to as snaking. The results shown in Figure 1 summarize numerical computations for the Swift–Hohenberg equation

$$U_t = -(1 + \partial_x^2)^2 U - \mu U + \nu U^2 - U^3, \quad x \in \mathbb{R}, \quad (1.1)$$

which is a variational system that is invariant under the reflection $x \mapsto -x$. The origin of the snaking diagram shown in Figure 1 was elucidated in [5, 18] through a comparison with two-dimensional Poincaré maps. These papers addressed only symmetric rolls, and it was not until [2] that the asymmetric roll patterns shown in Figure 1 were found for (1.1). Later, the existence of symmetric and asymmetric rolls was investigated independently in [4, 14], using formal beyond-all-orders expansions near the codimension-two point $(\mu, \nu) = (0, \sqrt{27/38})$, and in [1] using homoclinic bifurcation theory in a more abstract global framework.

The results in [1] are based on the idea that localized rolls can be constructed by gluing fronts and backs together as indicated in Figure 2. Writing the steady-state equation associated with (1.1) as the first-order ordinary differential equation

$$u_x = f(u, \mu), \quad u = (u_1, u_2, u_3, u_4) = (U, U_x, U_{xx}, U_{xxx}) \in \mathbb{R}^4, \quad (1.2)$$

we obtain a reversible Hamiltonian system, where reversibility is induced by the reflection $x \mapsto -x$, while the variational structure of (1.1) generates the Hamiltonian

$$H_0(u) = -\frac{\mu + 1}{2} u_1^2 - u_2^2 + \frac{u_3^2}{2} - u_2 u_4 + \int_0^{u_1} (\nu v^2 - v^3) dv. \quad (1.3)$$

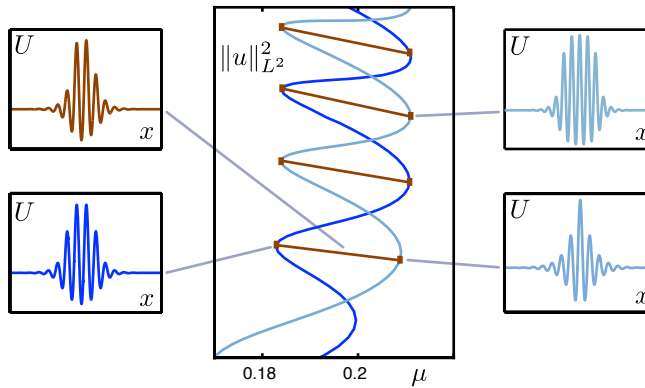


Figure 1: *Plotted is the numerically computed snaking bifurcation diagram of symmetric and asymmetric localized rolls of the Swift–Hohenberg equation (1.1) with $\nu = 1.6$. The insets contain representative solution profiles.*

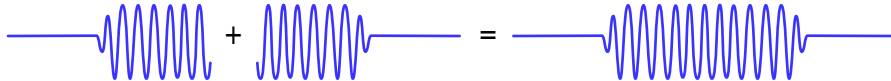


Figure 2: *A schematic figure that illustrates how localized roll structures can be obtained by gluing fronts and backs together.*

The system (1.2) can be analysed using homoclinic bifurcation theory by gluing the heteroclinic orbits that correspond to the fronts and backs in Figure 2 together to obtain homoclinic orbits that correspond to localized rolls. Underlying this analysis is the assumption that fronts and backs exist — a hypothesis that was verified formally in [4, 14] for (1.1). The Hamiltonian nature of (1.2) is helpful, as the dynamics can be reduced to a three-dimensional level set of the Hamiltonian, but, as shown in [1], not necessary. However, as pointed out in [10], it is not clear what happens in the case where the underlying partial differential equation is variational but not reversible. An example of such a system is the modified Swift–Hohenberg equation

$$U_t = -(1 + \partial_x^2)^2 U - \mu U + \nu U^2 - U^3 + \alpha U_x U_{xx}, \quad (1.4)$$

whose steady-state equation is not reversible for $\alpha \neq 0$ but admits the Hamiltonian $H(u) = H_0(u) + \frac{1}{3}\alpha u_x^3$ for all values of α in the variable u introduced in (1.2).

Our goal in this paper is to investigate whether snaking necessarily occurs for non-reversible conservative systems: our results show that there are two typical scenarios, one leading to snaking and the other one to bifurcation diagrams that consist entirely of bounded isolas. To prove this result, we will follow the analysis in [1, 10]. We remark that generic system without a conserved quantity, where heteroclinic cycles are of higher codimension, have been investigated previously in [3, 11, 12, 16, 17]. A numerical investigation of multi-pulses for non-reversible conservative systems can be found in [8]. Finally, we record that, while we were preparing this manuscript, Knobloch, Vielitz and Wagenknecht [13] have informed us that they obtained results similar to ours in a perturbative setting. The difference to our work is that they considered only small non-reversible conservative perturbations of a reversible conservative system; their methods are similar to ours except that their construction of solution branches relies on local continuation in the parameter that breaks the reversibility, while we determine the global structure of the solution set without the knowledge of any limiting reversibility structure.

The remainder of this paper is organized as follows. Section 2 contains the setup and the main result, which is then proved in §3. We end the paper in §4 with an outlook and a brief illustration of our results through numerical computations for two example systems, including (1.4).

2 Isolating versus snaking

Our interest is in four-dimensional conservative systems that exhibit heteroclinic orbits which connect a hyperbolic equilibrium to a hyperbolic periodic orbit and vice versa. Connecting orbits of this type are robust in conservative systems and will therefore exist in open regions in parameter space. We are interested in constructing homoclinic orbits from two such heteroclinic orbits. Our setup is close to that considered previously in [1] with the difference that we do not impose reversibility. Specifically, we make the following assumptions. We consider systems of the form

$$u_x = f(u, \mu), \quad (u, \mu) \in \mathbb{R}^4 \times \mathbb{R}, \quad (2.1)$$

where f is a smooth nonlinearity. Throughout, we assume that the parameter μ varies in a compact interval $J \subset \mathbb{R}$ with nonempty interior $\overset{\circ}{J}$. Our main structural assumption is that (2.1) is conservative.

Hypothesis (H1) *There exists a smooth function $H : \mathbb{R}^4 \times J \rightarrow \mathbb{R}$ with $H(0, \mu) = 0$ and $\langle f(u, \mu), \nabla H(u, \mu) \rangle = 0$ for all $(u, \mu) \in \mathbb{R}^4 \times J$.*

It is easy to see that (H1) implies that $H(u(x), \mu)$ is constant along solutions $u(x)$ of (2.1). Next, we discuss the existence of hyperbolic equilibria and periodic orbits. We assume that the origin is a hyperbolic saddle:

Hypothesis (H2) *The origin $u = 0$ is a hyperbolic equilibrium of (2.1) and $f_u(0, \mu)$ has two stable and two unstable eigenvalues for all $\mu \in J$.*

In conservative systems, periodic orbits arise typically in families that are parametrized by the value of the conserved quantity H . In particular, a periodic orbit within a given level set of H is usually isolated and robust, and we assume that this is the case inside the level set $H^{-1}(0)$ of (2.1) for each $\mu \in J$:

Hypothesis (H3) *Equation (2.1) admits a smooth family $\gamma(x, \mu)$ of periodic orbits with minimal periods $p(\mu) > 0$ so that $H(\gamma(x, \mu), \mu) = 0$ and $H_u(\gamma(x, \mu), \mu) \neq 0$ for all $x \in \mathbb{R}$ and $\mu \in J$ and so that $\gamma(x, \mu)$ has two positive Floquet multipliers $e^{-\alpha_s(\mu)p(\mu)}$ and $e^{\alpha_u(\mu)p(\mu)}$ with $\alpha_j(\mu) \geq \kappa > 0$ for $j = s, u$ uniformly in $\mu \in J$.*

We note that, unless the system is Hamiltonian, the two non-zero Floquet exponents $\alpha_{s,u}(\mu)$ of the periodic orbits in the level set $H^{-1}(0)$ are not necessarily related to each other. Since we assumed that the minimal periods are not zero, we can rescale time to normalize these periods so that $p(\mu) = 1$ for all $\mu \in J$, and we shall assume from now on that this normalization has been carried out. In particular, we can then parametrize the periodic orbits $\gamma(\varphi, \mu)$ using the phase φ that lives in $S^1 := \mathbb{R}/\mathbb{Z}$.

We now focus on heteroclinic orbits that connect $u = 0$ to the periodic orbit $\gamma(\cdot, \mu)$ or vice versa. Since H is conserved and $H(0, \mu) = 0$ for all μ , we can restrict our search for connecting orbits to the zero level set $H^{-1}(0)$ of H . Hypothesis (H3) implies that the zero level set of H is a three-dimensional manifold near each periodic orbit γ for each $\mu \in J$. The following lemma from [1] shows the existence of a smooth coordinate change in $H^{-1}(0)$ that puts (2.1) near the periodic orbits into normal form.

Lemma 1 ([1]) *Assume that Hypotheses (H1) and (H3) are met, then there exist a $\delta > 0$, a smooth change of coordinates near $\gamma(\cdot, \mu)$, and smooth real-valued functions h^c , h_j^s and h_j^u with $j = 1, 2$ so that (2.1) restricted to the zero level set of H is, for all $\mu \in J$, of the form*

$$\begin{aligned} v_x^c &= 1 + h^c(v, \mu)v^s v^u \\ v_x^s &= -[\alpha_s(\mu) + h_1^s(v, \mu)v^s + h_2^s(v, \mu)v^u]v^s \\ v_x^u &= [\alpha_u(\mu) + h_1^u(v, \mu)v^s + h_2^u(v, \mu)v^u]v^u, \end{aligned} \quad (2.2)$$

where $v = (v^c, v^s, v^u) \in S^1 \times I \times I$ with $S^1 = \mathbb{R}/\mathbb{Z}$ and $I = [-\delta, \delta]$. Note that $\gamma(\cdot, \mu)$ corresponds to $v = (v^c, 0, 0)$, where v^c can be thought of as the phase along the periodic orbit.

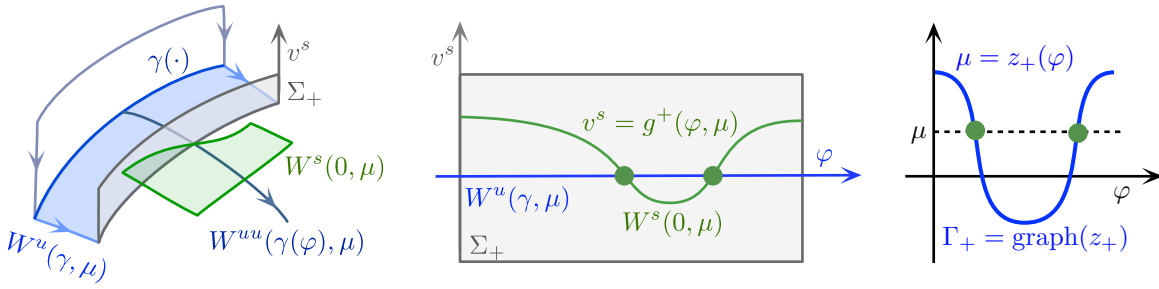


Figure 3: This schematic picture illustrates the notation introduced in Lemma 1 and Hypothesis (H4). The left and center panels illustrate the sections and invariant manifolds near the periodic orbits in the Fenichel coordinates of Lemma 1. The right panel shows the function z_+ and the associated set Γ_+ that encodes the phases associated with fronts: each filled circle in the (φ, v^s) -space in the center panel corresponds to a front that exists at the parameter value μ , which is then also encoded in the right panel as a filled circle in (φ, μ) -space.

We can now state our assumptions on the existence of heteroclinic orbits between the origin and the periodic orbits in the zero level set $H^{-1}(0)$. Using the Fenichel coordinates of Lemma 1 near the periodic orbit $\gamma(\cdot, \mu)$, we define the sections

$$\Sigma_- := S^1 \times \{v^s = \delta\} \times I, \quad \Sigma_+ := S^1 \times I \times \{v^u = \delta\}$$

as illustrated in Figure 3. Heteroclinic orbits that connect the origin to the periodic orbit lie in the intersection of the unstable manifold $W^u(0, \mu)$ of the origin and a strong stable fiber $W^{ss}(\gamma(\varphi, \mu), \mu)$ of the periodic orbit; similarly, connections between the periodic orbit and the origin lie in the intersection of the stable manifold $W^s(0, \mu)$ and a strong unstable fiber $W^{uu}(\gamma(\varphi, \mu), \mu)$. We therefore define the sets

$$\begin{aligned} \Gamma_- &:= \{(\varphi, \mu) \in S^1 \times J : W^u(0, \mu) \cap W^{ss}(\gamma(\varphi, \mu), \mu) \cap \Sigma_- \neq \emptyset\} \\ \Gamma_+ &:= \{(\varphi, \mu) \in S^1 \times J : W^s(0, \mu) \cap W^{uu}(\gamma(\varphi, \mu), \mu) \cap \Sigma_+ \neq \emptyset\}, \end{aligned}$$

which capture the parameter values μ and the phases φ for which such connections exist. For generic vector fields, the sets Γ_{\pm} are one-dimensional manifolds. For the sake of simplicity, we assume that these sets are given by graphs:

Hypothesis (H4) We assume that the sets Γ_{\pm} are the graphs of smooth 1-periodic functions $z_{\pm} : S^1 \rightarrow J$ so that $(\varphi, \mu) \in \Gamma_{\pm}$ if, and only if, $\mu = z_{\pm}(\varphi)$. Furthermore, we assume that there exist neighborhoods U_{\pm} of Γ_{\pm} in $S^1 \times J$, constants $\epsilon, \eta > 0$ and smooth functions $g^{\pm} : S^1 \times J \rightarrow I$ so that

$$\begin{aligned} \{(\varphi, \delta, v^u) \in W^u(0, \mu) \cap \Sigma_- : |v^u| < \epsilon, (\varphi, \mu) \in U_-\} &= \{(\varphi, \delta, g^-(\varphi, \mu)) : (\varphi, \mu) \in U_-\} \\ \{(\varphi, v^s, \delta) \in W^s(0, \mu) \cap \Sigma_+ : |v^s| < \epsilon, (\varphi, \mu) \in U_+\} &= \{(\varphi, g^+(\varphi, \mu), \delta) : (\varphi, \mu) \in U_+\} \end{aligned}$$

for each $\mu \in J$ and that $|g_{\mu}^{\pm}(\varphi, z_{\pm}(\varphi))| \geq \eta > 0$ for all $\varphi \in S^1$.

In other words, we assume that $W^u(0, \mu)$ intersects $W^{ss}(\gamma(\varphi, \mu), \mu)$ in Σ_- if, and only if, $g^-(\varphi, \mu) = 0$ or equivalently $\mu = z_-(\varphi)$, and similarly for connections between the periodic orbit and the origin. We also assume that the parameter μ moves the stable and unstable manifolds of the origin up and down relative to the invariant manifolds of the periodic orbits in the cross sections Σ_{\pm} . These assumptions can be relaxed significantly, and we refer to [1, §6.1] for details. Finally, we assume a nondegeneracy condition, namely that the functions z_{\pm} do not have any singular values in common (in particular, this assumption excludes systems that are reversible as these have $z_- = z_+$):

Hypothesis (H5) Whenever $z_-(\varphi_1) = z_+(\varphi_2)$, then $z'_-(\varphi_1)$ and $z'_+(\varphi_2)$ do not both vanish.

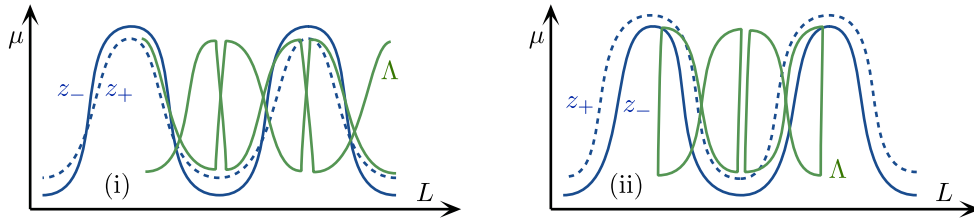


Figure 4: The panels illustrate the two cases considered in Theorem 1: in each case, the bifurcation branches Λ of homoclinic orbits are constructed from the shown sample graphs of z_{\pm} using the characterization of Λ given in Theorem 1(i). Panel (i) shows the snaking scenario covered in Theorem 1(ii), while panel (ii) corresponds to the non-snaking case discussed in Theorem 1(iii). Note that these two cases occur naturally when perturbing the snaking diagram of the reversible Swift–Hohenberg equation that we reviewed in Figure 1.

Our goal is to construct homoclinic orbits to the origin by gluing the heteroclinic orbits between the origin and the periodic orbits $\gamma(\cdot, \mu)$ together. In particular, the homoclinic orbits constructed in this fashion will pass exactly once near the periodic orbits and spend a long time during their passage. We associate with each such homoclinic orbit the time $2L$ that the orbit spends between the incoming section Σ_- and the outgoing section Σ_+ : using the original motivation of capturing localized patterns that contain a long plateau formed by periodic patterns, we will refer to these times L as the width of the homoclinic orbits.

We will show below that homoclinic orbits with the above properties arise as smooth branches in $C^1(\mathbb{R}, \mathbb{R}^4) \times \mathring{J}$ that can be parametrized by their arclength. In particular, for each such branch, we can then consider the function $s \mapsto L(s)$ that associates to each homoclinic orbit its width. We say that snaking occurs if there is a branch of homoclinic orbits so that the associated widths $L(s)$ increase without bound. Conversely, we say that the bifurcating branches consist of isolas (or that snaking does not occur) if the function $L(s)$ associated with each branch of homoclinic orbits is bounded uniformly along the branch. In the following theorem, we characterize branches of homoclinic orbits and give conditions for snaking and non-snaking.

Theorem 1 *If Hypotheses (H1)-(H5) are met, then there is a constant $L_0 \gg 1$ such that the following is true:*

- (i) *Equation (2.1) has a homoclinic orbit of width $L_* > L_0$ that passes exactly once near the periodic orbits from (H3) for the parameter value μ_* if, and only if,*

$$(\mu_*, L_*) \in \Lambda := \{(\mu, L) : \exists \varphi \in [0, 1] \text{ such that } \mu = z_-(\varphi - L), z_-(\varphi - L) = z_+(\varphi + L)\},$$

and there is exactly one such homoclinic orbit for each $(\mu_, L_*) \in \Lambda$.*

- (ii) *If $\max z_+ > \max z_- \geq \min z_- > \min z_+$, then there is a branch of homoclinic orbits along which $L(s)$ increases without bound: thus, snaking occurs.*
- (iii) *If $\max z_+ > \max z_-$ and $\min z_+ > \min z_-$, then $L(s)$ is bounded along each branch of homoclinic orbits: thus, each branch is an isola.*

These statements remain true if z_{\pm} are interchanged in the inequalities that appear in (ii) and (iii).

The two scenarios outlined in Theorem 1 are illustrated in Figure 4 for functions $z_{\pm}(\varphi)$ that can be thought of as two specific small perturbations of the function $z(\varphi)$ that corresponds to the reversible Swift–Hohenberg equation. In particular, Figure 4(i) shows that there are precisely two unbounded branches in the case of Theorem 1(ii) and that these are formed by following alternately the symmetric and asymmetric branches as L increases. In the case described in Theorem 1(iii), the bounded branches are also composed of the symmetric and asymmetric branches, but the branches reconnect in such a way that each resulting bifurcation curve is closed. The differences between these cases are due to the different unfolding of the pitchfork bifurcations at the intersection of the symmetric and asymmetric branches that is created by the specific symmetry-breaking perturbation.

3 Proof of Theorem 1

We are interested in constructing homoclinic orbits to the origin that pass precisely once near the periodic orbits $\gamma(\cdot, \mu)$. Using the coordinates and notation introduced in Lemma 1, we therefore seek a sufficiently large constant $L \gg 1$, a parameter $\mu \in J$, and a solution $v(x)$ of (2.2) on the interval $[-L, L]$ such that

$$v(-L) \in W^u(0, \mu) \cap \Sigma_-, \quad v(L) \in W^s(0, \mu) \cap \Sigma_+, \quad v(x) \in S^1 \times I \times I \quad \text{for } x \in [-L, L]. \quad (3.1)$$

The initial steps of the analysis given below follow closely the strategy presented earlier in [1, 10]. We begin by stating a result that can be proved as in [1, Lemma 3.1]: this lemma provides a characterization and an expansion of solutions $v(x)$ of (2.2) that will allow us to state the matching conditions (3.1) in a more explicit form.

Lemma 2 ([1]) *There exist positive constants L_0 and κ so that the following is true: For each $L > L_0$, $\varphi \in S^1$, and $\mu \in J$, equation (2.2) has a unique solution $v(x) = v(x, \varphi, \mu)$ that is defined for $x \in [-L, L]$ with*

$$v(-L) \in \Sigma_-, \quad v(L) \in \Sigma_+, \quad v^c(0) = \varphi, \quad v(x) \in S^1 \times I \times I \quad \forall x \in [-L, L].$$

Furthermore, we have the expansions

$$\begin{aligned} v(-L) &= (\varphi - L + O(e^{-\kappa L}), \delta, O(e^{-\kappa L})) \\ v(L) &= (\varphi + L + O(e^{-\kappa L}), O(e^{-\kappa L}), \delta) \\ v(0) &= (\varphi, O(e^{-\kappa L}), O(e^{-\kappa L})), \end{aligned} \quad (3.2)$$

and the error estimates in (3.2) are smooth in (L, φ, μ) .

Using the existence and uniqueness part of Lemma 2 together with the representation of the intersections of the stable and unstable manifolds of the origin with the sections Σ_{\pm} provided in Hypothesis (H4), we see that (3.1) is equivalent to finding solutions $(L, \varphi, \mu) \in \mathbb{R}^+ \times S^1 \times J$ with $L \gg 1$ of the system

$$g^-(v^c(-L, \varphi, \mu), \mu) = v^u(-L, \varphi, \mu), \quad g^+(v^c(L, \varphi, \mu), \mu) = v^s(L, \varphi, \mu). \quad (3.3)$$

Substituting the expansion (3.2) into (3.3), and using that the functions g^{\pm} are smooth and defined on the compact set $S^1 \times J$, we arrive at the equivalent system

$$g^-(\varphi - L, \mu) = O(e^{-\kappa L}), \quad g^+(\varphi + L, \mu) = O(e^{-\kappa L}), \quad (3.4)$$

where the remainder terms are smooth in (L, φ, μ) . The idea is now to solve one of the two equations in (3.4) for μ as a function of L : which one we solve does not matter, and we choose to solve the first equation.

Lemma 3 *There exists an $L_0 \gg 1$ such that the first equation in (3.4), given by*

$$g^-(\varphi - L, \mu) = O(e^{-\kappa L}), \quad (3.5)$$

has a unique solution $\mu = \mu_*(L, \varphi) \in J$ for each $(L, \varphi) \in (L_0, \infty) \times S^1$ and

$$\mu_*(L, \varphi) = z_-(\varphi - L) + O(e^{-\kappa L}).$$

Proof. By Hypothesis (H4), we have $g^-(\varphi, \mu) = 0$ if, and only if, $\mu = z_-(\varphi)$. Thus, (3.5) has a solution for $L \gg 1$ if, and only if, μ is close to $z_-(\varphi - L)$. Hence, we write $\mu = z_-(\varphi - L) + \tilde{\mu}$ and obtain the equation

$$G^-(L, \varphi, \tilde{\mu}) := g^-(\varphi - L, z_-(\varphi - L) + \tilde{\mu}) - O(e^{-\kappa L}) = 0. \quad (3.6)$$

Since

$$G^-(L, \varphi, 0) = O(e^{-\kappa L}), \quad G_{\tilde{\mu}}^-(L, \varphi, 0) = g_{\tilde{\mu}}^-(\varphi - L, z_-(\varphi - L)) + O(e^{-\kappa L}),$$

and $|g_{\tilde{\mu}}^-(\varphi, z_-(\varphi))| \geq \eta > 0$ uniformly in $\varphi \in S^1$ by Hypothesis (H4), we can solve (3.6) uniquely for $\tilde{\mu}$ near zero as a function $\tilde{\mu} = \tilde{\mu}_*(L, \varphi)$ for $(L, \varphi) \in \mathbb{R}^+ \times J$ with $L \gg 1$. Furthermore, $\tilde{\mu}_*(L, \varphi) = O(e^{-\kappa L})$, which completes the proof. \blacksquare

Having solved the first equation in (3.4), it remains to solve the second equation

$$g^+(\varphi + L, \mu_*(L, \varphi)) = O(e^{-\kappa L}).$$

Substituting the expression for $\mu_*(L, \varphi)$ and using that g^+ is smooth and defined on the compact set $S^1 \times J$, we arrive at the equation

$$G^+(L, \varphi) := g^+(\varphi + L, z_-(\varphi - L)) - O(e^{-\kappa L}) = 0 \quad (3.7)$$

that we need to solve for $L \gg 1$ and $\varphi \in S^1$. We define the functions

$$Z, G_0^+ : (L_0, \infty) \rightarrow \mathbb{R}, \quad Z(L, \varphi) := z_-(\varphi - L) - z_+(\varphi + L), \quad G_0^+(L, \varphi) := g^+(\varphi + L, z_-(\varphi - L))$$

and note that both functions are 1-periodic in each of their arguments L and φ . In particular, the set

$$[G_0^+]^{-1}(0) \stackrel{\text{(H4)}}{=} Z^{-1}(0) = \{(L, \varphi) : z_-(\varphi - L) = z_+(\varphi + L), L > L_0\} \subset (L_0, \infty) \times S^1$$

has the property that $(L, \varphi) \in Z^{-1}(0)$ if, and only if, $(L + 1, \varphi) \in Z^{-1}(0)$ for $L > L_0$. The following lemma shows that $Z^{-1}(0)$ and $[G^+]^{-1}(0)$ are smooth manifolds that are diffeomorphic to each other and $O(e^{-\kappa L_0})$ close in C^1 .

Lemma 4 *There exist constants $L_0 \gg 1$ and $\eta_0 > 0$ such that*

$$|\nabla Z(L, \varphi)| + |\nabla G_0^+(L, \varphi)| + |\nabla G^+(L, \varphi)| \geq \eta_0 > 0, \quad G^+(L, \varphi) = O(e^{-\kappa L})$$

for all $(L, \varphi) \in Z^{-1}(0)$. Furthermore, $Z^{-1}(0)$ and $[G^+]^{-1}(0)$ are one-dimensional submanifolds of $(L_0, \infty) \times S^1$ without boundary that are diffeomorphic and $O(e^{-\kappa L_0})$ close to each other in C^1 .

Proof. We have

$$\nabla Z(L, \varphi) = \begin{pmatrix} -1 & -1 \\ 1 & -1 \end{pmatrix} \begin{pmatrix} z'_-(\varphi - L) \\ z'_+(\varphi + L) \end{pmatrix},$$

and Hypothesis (H5) implies that $\nabla Z(L, \varphi) \neq 0$ for all $(L, \varphi) \in Z^{-1}(0)$ since we have $z_-(\varphi - L) = z_+(\varphi + L)$ for such (L, φ) . Since Z is 1-periodic in each argument, its gradient on $Z^{-1}(0)$ is then uniformly bounded away from zero. Next, we note that $g^+(\varphi, z_+(\varphi)) \equiv 0$ implies that

$$g_{\varphi}^+(\varphi, z_+(\varphi)) = -g_{\mu}^+(\varphi, z_+(\varphi))z'_+(\varphi) \quad (3.8)$$

for all $\varphi \in S^1$. Using this identity, we obtain for each $(L, \varphi) \in Z^{-1}(0)$, that is for each (L, φ) for which $z_-(\varphi - L) = z_+(\varphi + L)$, that

$$\begin{aligned} \nabla G_0^+(L, \varphi) &= \begin{pmatrix} g_{\varphi}^+(\varphi + L, z_-(\varphi - L)) - g_{\mu}^+(\varphi + L, z_-(\varphi - L))z'_-(\varphi - L) \\ g_{\varphi}^+(\varphi + L, z_-(\varphi - L)) + g_{\mu}^+(\varphi + L, z_-(\varphi - L))z'_-(\varphi - L) \end{pmatrix} \\ &= \begin{pmatrix} g_{\varphi}^+(\varphi + L, z_+(\varphi + L)) - g_{\mu}^+(\varphi + L, z_+(\varphi + L))z'_-(\varphi - L) \\ g_{\varphi}^+(\varphi + L, z_+(\varphi + L)) + g_{\mu}^+(\varphi + L, z_+(\varphi + L))z'_-(\varphi - L) \end{pmatrix} \\ &\stackrel{(3.8)}{=} g_{\mu}^+(\varphi + L, z_+(\varphi + L)) \begin{pmatrix} -1 & -1 \\ 1 & -1 \end{pmatrix} \begin{pmatrix} z'_-(\varphi - L) \\ z'_+(\varphi + L) \end{pmatrix} \\ &= g_{\mu}^+(\varphi + L, z_+(\varphi + L)) \nabla Z(L, \varphi). \end{aligned}$$

Since $|g_{\mu}^+(\varphi, z_+(\varphi))| \geq \eta > 0$ for all $\varphi \in S^1$ by Hypothesis (H4), the statements about the gradients follow easily. The remaining claims are a consequence of the implicit function theorem. \blacksquare

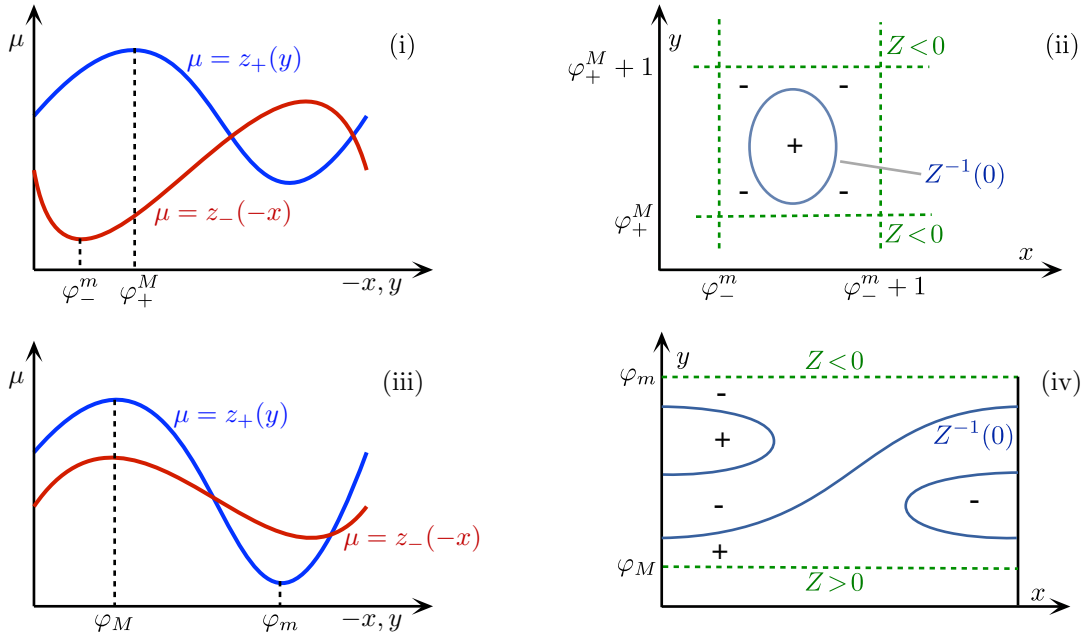


Figure 5: Panels (i) and (iii) to the left contain the graphs of typical functions z_{\pm} that satisfy the conditions (3.9) and (3.10), respectively. The panels (ii) and (iv) to the right illustrate the resulting level sets $Z^{-1}(0)$ of the function $Z(x, y) := z_{-}(-x) - z_{+}(y)$. In the top row, note that $Z(x, y) < 0$ when $-x = \varphi_{-}^m$ or when $y = \varphi_{+}^M$, and since Z is 1-periodic in each of its arguments, the connected components of $Z^{-1}(0)$ are bounded. In the bottom row, for each fixed x , $Z(x, y)$ changes from positive to negative as y varies from φ_M to φ_m ; this implies that not all connected components of $Z^{-1}(0)$ can be bounded.

It remains to explore the structure of the one-dimensional manifold $Z^{-1}(0)$ and investigate under which conditions it contains connected components that are unbounded in $(L_0, \infty) \times S^1$. We set $(x, y) := (L - \varphi, L + \varphi) \in \mathbb{R}^2$ and define, with a slight abuse of notation, $Z(x, y) := z_{-}(-x) - z_{+}(y)$. As shown above, $Z^{-1}(0)$ consists of smooth curves without boundary that can be parameterized by their arclength, which we denote by s . We refer to these smooth curves, which coincide with the connected components of $Z^{-1}(0)$, as branches.

Assume first that

$$\max z_{+} > \max z_{-} \quad \text{and} \quad \min z_{+} > \min z_{-}. \quad (3.9)$$

We pick φ_{+}^M and φ_{-}^m such that $z_{+}(\varphi_{+}^M + \ell) > z_{-}(x)$ and $z_{+}(y) > z_{-}(-\varphi_{-}^m + k)$ for all $x, y \in \mathbb{R}$ and $k, \ell \in \mathbb{Z}$. In particular, as illustrated in Figure 5(i), we have $Z(x, \varphi_{+}^M + \ell) < 0$ and $Z(\varphi_{-}^m + k, y) < 0$ for all $x, y \in \mathbb{R}$ and $k, \ell \in \mathbb{Z}$, which demonstrates that any branch $(x(s), y(s))$ in $Z^{-1}(0)$ must necessarily be bounded. Hence, we conclude that $(x(s), y(s))$ must lie on a closed curve and that $2L(s) = x(s) + y(s)$ is bounded along this curve. This proves Theorem 1(iii).

Next, assume that

$$\max z_{+} > \max z_{-} \geq \min z_{-} > \min z_{+}. \quad (3.10)$$

Pick $\varphi_{m, M}$ such that $z_{+}(\varphi_M) = \max z_{+}$ and $z_{+}(\varphi_m) = \min z_{+}$. Without loss of generality, we may assume that $0 < \varphi_m < \varphi_M < 1$. We conclude that $Z(x, \varphi_M) < 0$ and $Z(x, \varphi_m) > 0$ for all $x \in \mathbb{R}$. Hence, if we define the strip $\Omega := \mathbb{R} \times [\varphi_m, \varphi_M]$, then $Z^{-1}(0)$ cannot intersect the boundary of Ω , and $Z^{-1}(0) \cap \Omega$ is not empty. We focus on branches $(x(s), y(s))$ in $Z^{-1}(0) \cap \Omega$; the other case, where $\varphi_M < y(s) < \varphi_m + 1$, can be dealt with analogously. Thus, assume that $(x(s), y(s)) \in Z^{-1}(0) \cap \Omega$ for all s . If $x(s)$ is bounded, then, using that $|\nabla Z(x, y)| \geq \eta_0 > 0$ on $Z^{-1}(0)$, it is easy to see that the branch is a closed curve. We claim that there exists at least one branch in $Z^{-1}(0) \cap \Omega$ such that $x(s)$ is unbounded; since $y(s)$ is always bounded, this would imply that $2L(s) = x(s) + y(s)$ is unbounded and complete the proof of Theorem 1(ii).

To prove this claim, we can assume that $z'_+(y) \neq 0$ for all $(0, y) \in Z^{-1}(0) \cap \Omega$; otherwise, consider $x = \epsilon$ for an appropriate value of ϵ near zero. In particular, as indicated in Figure 5(ii), each branch in $Z^{-1}(0) \cap \Omega$ crosses the interval $x = 0$ transversally, and $Z(0, y)$ changes sign across each branch when varying y from φ_m to φ_M . Since $Z(0, \varphi_m) > 0 > Z(0, \varphi_M)$, we conclude that an odd number of branches in $Z^{-1}(0) \cap \Omega$ cross $x = 0$. Furthermore, since each bounded branch corresponds to a closed curve in $Z^{-1}(0)$, each bounded branch in $Z^{-1}(0) \cap \Omega$ intersects $x = 0$ an even number of times. Taken together, this implies that there is an odd, and hence nonzero, number of unbounded branches in $Z^{-1}(0) \cap \Omega$ that intersect $x = 0$, which completes the proof of Theorem 1(iii).

4 Numerical simulations, and outlook

We illustrate our results by investigating the systems

$$\begin{pmatrix} \dot{u}_1 \\ \dot{u}_2 \\ \dot{u}_3 \\ \dot{u}_4 \end{pmatrix} = \begin{pmatrix} u_2 \\ u_3 \\ u_4 \\ -(1 + \mu)u_1 - 2u_3 + \nu u_1^2 - u_1^3 + \alpha u_2 u_3 \end{pmatrix} \quad (4.1)$$

and

$$\begin{pmatrix} \dot{u}_1 \\ \dot{u}_2 \\ \dot{u}_3 \\ \dot{u}_4 \end{pmatrix} = \begin{pmatrix} u_2 \\ u_3 \\ u_4 \\ -(1 + \mu)u_1 - 2u_3 + \nu u_1^2 - u_1^3 + \alpha u_2 (3u_3 \sin u_3 + u_2 u_4 \cos u_3) \end{pmatrix}. \quad (4.2)$$

Neither of these systems is reversible for $\alpha \neq 0$, but they are conservative with respect to the functions $H(u) = H_0(u) + \frac{1}{3}\alpha u_2^3$ and $H(u) = H_0(u) + \alpha u_2^3 \sin u_3$, respectively, where $H_0(u)$ has been defined in (1.3). We used AUTO-07P [7] to calculate homoclinic orbits of (4.1) and (4.2) for $(\nu, \alpha) = (1.6, 0.15)$ and continue them in μ . The results are shown in Figure 6, and we see that (4.1) gives unbounded branches, while (4.2) exhibits isolas. Figure 7 contains additional computations for (4.1) at $(\nu, \alpha) = (1.6, 0.1)$ and, specifically, a comparison with the snaking and ladder branches for $\alpha = 0$. The resulting bifurcation diagram closely resembles Figure 4(i), and the branch for $\alpha = 0.1$ switches back and forth between the two symmetric branches of the $\alpha = 0$ system by using the asymmetric branches as bridges. As mentioned earlier, the pitchfork bifurcations from symmetric to asymmetric profiles that are present in the reversible system are no longer generic for non-reversible systems: instead, the symmetry-breaking terms break the pitchfork branches up into a saddle-node branch and a second branch that does not undergo any bifurcation. Globally, the resulting branch structure can arrange itself in two different ways, one leading to isolas as in Figure 6(ii) and the other one to the snaking diagram visible in Figure 6(i).

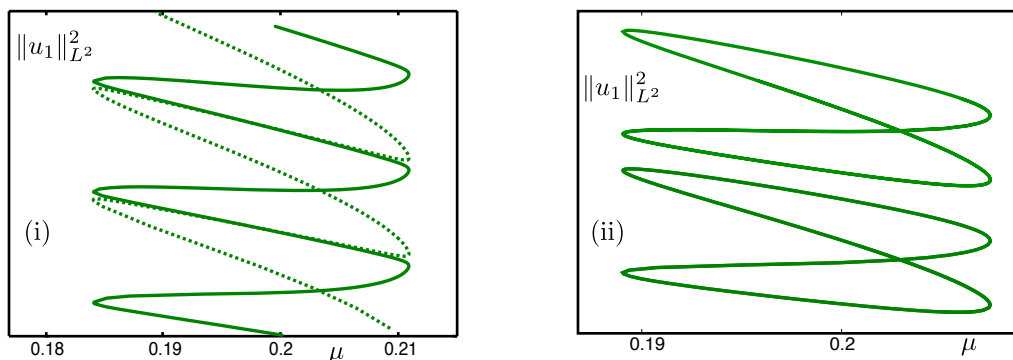


Figure 6: Panel (i) contains two unbounded branches of localized rolls of (4.1), while panel (ii) contains two isolas of localized rolls of (4.2). The parameters are $(\nu, \alpha) = (1.6, 0.15)$.

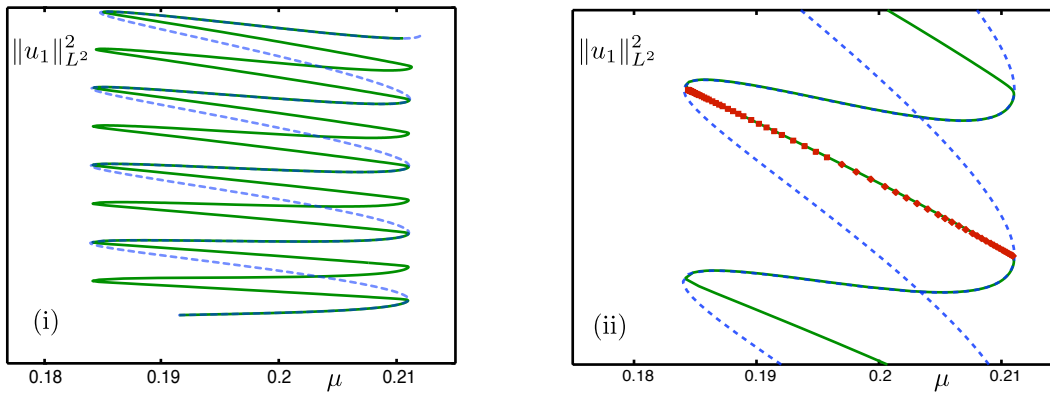


Figure 7: Panel (i) contains a branch of localized rolls of (4.1) with $(\nu, \alpha) = (1.6, 0.1)$ (solid green curve) and a branch of symmetric localized rolls of (1.1) (dashed blue curve). The close-up in panel (ii) contains the two symmetric branches (dashed blue) and one of the asymmetric branches (red crosses) of (1.1) from Figure 1 together with the branch of localized rolls of (4.1) (solid green).

Finally, we review briefly our hypotheses and discuss open problems. We restricted ourselves to the case where the sets Γ_{\pm} of phases φ and parameter values μ for which connecting orbits between the origin and periodic orbits exist are graphs of the form $\mu = z_{\pm}(\varphi)$. This assumption is not necessary, and it is straightforward to use the arguments presented in [1, §6.1] to generalize our results to the case where the sets Γ_{\pm} are arbitrary one-dimensional manifolds. When the nondegeneracy condition (H5) fails, then, generically, two branches will touch, form a cross, and subsequently rearrange themselves: this is a codimension-one scenario that can be analysed as well under additional unfolding conditions.

This paper dealt with snaking scenarios in non-reversible conservative systems, including perturbative settings where small non-reversible terms are added to a reversible system. Reversible nonconservative systems had been investigated previously in [1, §6.4]. It is natural to ask what happens when both structures are broken: in this case, the family of periodic orbits that is present for reversible or conservative systems will generically break up into finitely many isolated periodic orbits. Fenichel coordinates could still be used to describe the slow dynamics along the center manifold near the original family of periodic orbit, and a comprehensive snaking analysis should certainly be possible. It would also be interesting to investigate the effects of nonhomogeneous x -dependent terms on snaking: in [15], a rich bifurcation structure was found numerically for radial spots in the planar Swift–Hohenberg equation, which could be studied analytically by focusing on the radial system in the non-integer dimension $1 + \epsilon$ with $0 < \epsilon \ll 1$.

Acknowledgments. Sandstede was partially supported by the NSF through grant DMS-0907904. Xu was supported by a fellowship of the Chinese Scholarship Council and by the Science Foundation of Zhejiang Province through grant Y610081.

References

- [1] M. Beck, J. Knobloch, D. J. B. Lloyd, B. Sandstede and T. Wagenknecht. Snakes, ladders, and isolas of localized patterns. *SIAM J. Math. Anal.* **41** (2009) 936–972.
- [2] J. Burke and E. Knobloch. Localized states in the generalized Swift–Hohenberg equation. *Phys. Rev. E* **73** (2006) 056211.
- [3] A. R. Champneys, V. Kirk, E. Knobloch, B. E. Oldeman and J. D. M. Rademacher. Unfolding a tangent equilibrium-to-periodic heteroclinic cycle. *SIAM J. Appl. Dyn. Syst.* **8** (2009) 1261–1304.

- [4] S. J. Chapman and G. Kozyreff. Exponential asymptotics of localised patterns and snaking bifurcation diagrams. *Physica D* **238** (2009) 319–354.
- [5] P. Couillet, C. Riera and C. Tresser. Stable static localized structures in one dimension. *Phys. Rev. Lett.* **84** (2000) 3069–3072.
- [6] J. H. P. Dawes. The emergence of a coherent structure for coherent structures: localized states in nonlinear systems. *Phil. Trans. R. Soc. A* **368** (2010) 3519–3534.
- [7] E. J. Doedel and B. E. Oldeman. *AUTO-07P: Continuation and bifurcation software for ordinary differential equations*. Technical report, Concordia University, 2009.
- [8] S. M. Houghton and T. Wagenknecht. Multi-pulses in the Swift–Hohenberg equation with broken symmetry. In preparation (2012).
- [9] E. Knobloch. Spatially localized structures in dissipative systems: open problems. *Nonlinearity* **21** (2008) T45–T60.
- [10] J. Knobloch, D. J. B. Lloyd, B. Sandstede and T. Wagenknecht. Isolats of 2-pulse solutions in homoclinic snaking scenarios. *J. Dynam. Differ. Eqns.* **23** (2011) 93–114.
- [11] J. Knobloch and T. Rieß. Lin’s method for heteroclinic chains involving periodic orbits. *Nonlinearity* **23** (2010) 23–54.
- [12] J. Knobloch, T. Rieß and M. Vielitz. Nonreversible homoclinic snaking. *Dynamical Systems* **26** (2011) 335–365.
- [13] J. Knobloch, M. Vielitz and T. Wagenknecht. Nonreversible perturbations of homoclinic snaking scenarios. Preprint, 2012.
- [14] G. Kozyreff and S. J. Chapman. Asymptotics of large bound states of localised structures. *Phys. Rev. Lett.* **97** (2006) 044502.
- [15] S. McCalla and B. Sandstede. Snaking of radial solutions of the multi-dimensional Swift-Hohenberg equation: a numerical study. *Physica D* **239** (2010) 1581–1592.
- [16] J. D. M. Rademacher. Homoclinic orbits near heteroclinic cycles with one equilibrium and one periodic orbit. *J. Differ. Eqns.* **218** (2005) 390–443.
- [17] J. D. M. Rademacher. Lyapunov–Schmidt reduction for unfolding heteroclinic networks of equilibria and periodic orbits with tangencies. *J. Differ. Eqns.* **249** (2010) 305–348.
- [18] P. D. Woods and A. R. Champneys. Heteroclinic tangles and homoclinic snaking in the unfolding of a degenerate reversible Hamiltonian Hopf bifurcation. *Physica D* **129** (1999) 147–170.